JOC The Journal of Organic Chemistry

Article

pubs.acs.org/joc

Synthesis and Characterization of Two Unsymmetrical Indenofluorene Analogues: Benzo[5,6]-*s*-indaceno[1,2-*b*]thiophene and Benzo[5,6]-*s*-indaceno[2,1-*b*]thiophene

Jonathan L. Marshall, Nathaniel J. O'Neal, Lev N. Zakharov, and Michael M. Haley*

Department of Chemistry & Biochemistry and Materials Science Institute, University of Oregon, Eugene, Oregon 97403-1253, United States

Supporting Information

ABSTRACT: The synthesis and characterization of two benzo-indaceno-thiophene compounds (*anti*-BIT and *syn*-BIT) are described. Two sequential Suzuki cross-couplings utilizing the halogen selectivity of this reaction permit modular assembly of unsymmetrical indeno[1,2-*b*]fluorene analogues. Analysis of their cyclic voltammetry and UV−vis spectra reveal that the optical and electrochemical properties of the BITs lie between those of indeno[1,2-*b*]fluorenes and indacenodithiophene.

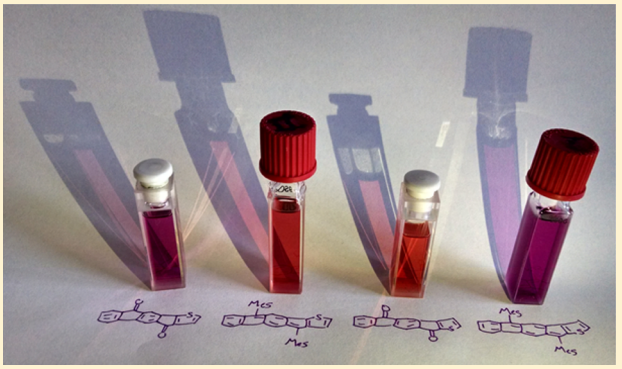

INTRODUCTION

Indenofluorenes (IFs) are an interesting class of cyclopentane-fused hydrocarbons that have been the focus of interest of our lab,[1−14] as well as others,[15−26] over the last five years. In addition to pure hydrocarbon structures, such as IFs **1a**,**b**, variants containing thiophene, such as indacenodithiophene (*anti*-IDT **2a**, *syn*-IDT **3a**) or indacenodibenzothiophene (*anti*-IDBT **2b**, *syn*-IDBT **3b**), and selenophene, such as indacenodiselenophene (IDS **2c**), have also recently been disclosed (Figure 1).[8,13,14,16] Structurally similar to pentacene, the inclusion of two carbonaceous, fully conjugated five-membered rings, such as in **1a**,**b**, **2a**−**c**, or **3a**,**b**, impart an intrinsic ability to accept electrons.[1−3,8,14] We have explored both substitution of the IFs at the 2- and 8-positions (e.g., **1a**)[2] or 6- and 12-positions (**1b**)[1] with some variations of **1b** displaying amphoteric redox behavior. It should be noted that, in all cases for IFs and related structures, the current synthetic methods for outer ring substitution or core construction limit us to C_{2h} symmetric compounds.

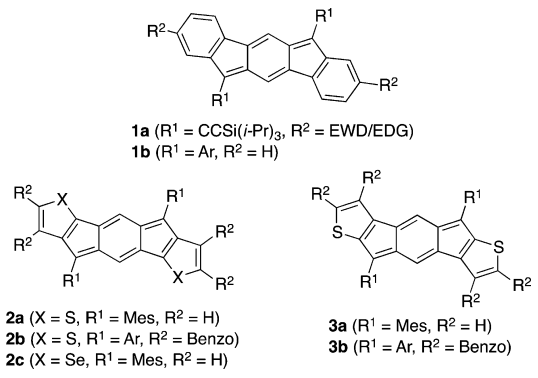

Figure 1. Indenofluorenes (**1a**,**b**) and related heterocyclic congeners (**2a**−**c**, **3a**,**b**).

Conjugated polycyclic hydrocarbons have captivated chemists' imagination over the last two decades due to their interesting optoelectronic properties and application in organic electronics.[27−40] Research into acenes for use in organic electronics has focused on tuning their optoelectronic properties while at the same time optimizing the solid-state structure to maximize intermolecular interactions.[32,34,41,42] Recently, desymmetrization (breaking the D_{2v} or C_{2h} symmetry of typical acenes) has been used as a means of creating a dipole moment (**4** and **5**, Figure 2) and exploiting this property to influence solid-state packing. Others have utilized the desymmetrization of acenes to tune electronics (**5** and **6**).[43−50] Despite the promise of these unsymmetrical acenes, their study is fairly limited given their compound specific and often difficult preparation.

As the synthesis of IFs and related structures utilizes a Suzuki cross-coupling to attach various aryl rings to what will eventually become the *s*-indacene core, we anticipated that the halogen selectivity of this reaction could be used to desymmetrize IFs in a modular fashion. By desymmetrizing the IFs, we gain access not only to derivatives that could utilize a

Received: February 15, 2016
Published: March 25, 2016

DOI: 10.1021/acs.joc.6b00340
J. Org. Chem. 2016, 81, 3674−3680

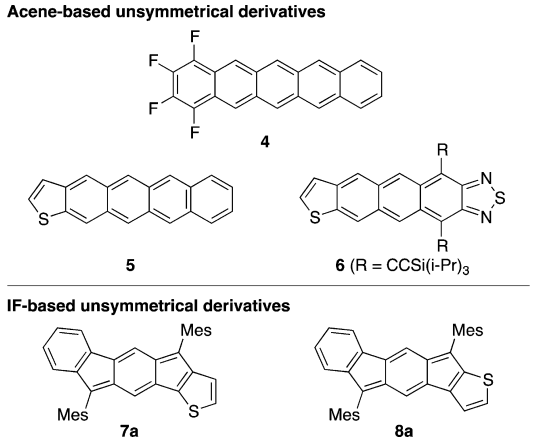

Figure 2. Unsymmetric acenes **4**–**6** and unsymmetric IF analogues *anti*-BIT **7a** and *syn*-BIT **8a**.

dipole to influence the solid-state packing, but we also access a powerful new strategy to study electronic communication through the IF core via donor–acceptor and cruciform topologies. As a proof of concept, we have developed a modular synthesis via sequential Suzuki cross-couplings from diethyl 2-bromo-5-chloroterephthalate **9** for the preparation of new unsymmetrical IF analogues benzo[5,6]-*s*-indaceno[1,2-*b*]thiophene (*anti*-BIT **7a**,**b**) and benzo[5,6]-*s*-indaceno[2,1-*b*]thiophene (*syn*-BIT **8a**–**c**).

RESULTS AND DISCUSSION

Symmetric IFs and their congeners are usually prepared by Pd-mediated cross-coupling of aryl boronic acids to 1,4-dibromo-2,5-dimethylbenzene or diethyl 2,5-dibromoterephthalate. Intramolecular Friedel–Crafts acylation of the resultant *p*-terphenyl derivatives provide the corresponding diones that can be elaborated further into the fully conjugated IF/IDT/IDBT/IDS via nucleophilic addition of aryl or ethynyl groups followed by a $SnCl_2$-mediated reductive dearomatization. Utilizing diethyl 2-bromo-5-chloroterephthalate (**9**, Scheme 1) allows us to perform sequential and selective Suzuki–Miyaura cross-coupling reactions to attach a variety of different aryl groups to the IF core. Surprisingly, outside of a few patents, the precursor to **9**, 1-bromo-4-chloro-2,5-dimethylbenzene (**10**), is poorly represented in the literature.[51,52] Bromination of commercially available 2-chloro-1,4-dimethylbenzene (**11**) furnishes **10**, which in turn is readily converted to terephthalate **9** via $KMnO_4$ oxidation followed by Fischer esterification to provide the key cross-coupling partner in excellent yield on 15 g scale. With **9** in hand, standard Suzuki–Miyaura conditions afford biphenyl **12**. Switching to the more activating SPhos ligand permits cross-coupling of either 2- or 3-thienylboronic acid to furnish diesters **13** or **14**, respectively.[53] Saponification followed by conversion to the acid chloride and finally a Friedel–Crafts acylation provides the BIT-diones **15** and **16** in good overall yields on gram scale. Surprisingly, unlike other IF-diones synthesized in our lab, **15** and **16** were appreciably soluble in a variety of chlorinated and aromatic solvents. We ascribe this to the unsymmetrical nature of the diones and the slight dipole moment this imparts. Treatment of dione **15** with mesitylmagnesium bromide followed by $SnCl_2$-mediated reductive dearomatization in degassed toluene gratifyingly furnished *anti*-BIT **7a**, and treatment of dione **16** with mesityllithium (via *t*-BuLi and bromomesitylene) followed by the $SnCl_2$ reaction provided *syn*-BIT **8a**.

Surprisingly, both diones **15** and **16** showed unexpected reactivity to the nucleophilic source used. Treatment of **15** with mesityllithium (via *n*-BuLi and bromomesitylene) did not yield *anti*-BIT **7a** but rather yielded *anti*-BIT **7b** (see Supporting Information (SI) for the crystal structure of **7b**). We believe that mesityllithium was sufficient to deprotonate the dione (or some intermediate structure) at the α-position of the thiophene ring and that this deprotonated species reacted with 1-bromobutane (produced by the lithium-halogen exchange with bromomesitylene) to eventually yield the butylated *anti*-

Scheme 1. Synthesis of *anti*-BITs 7a,b and *syn*-BITs 8a–c

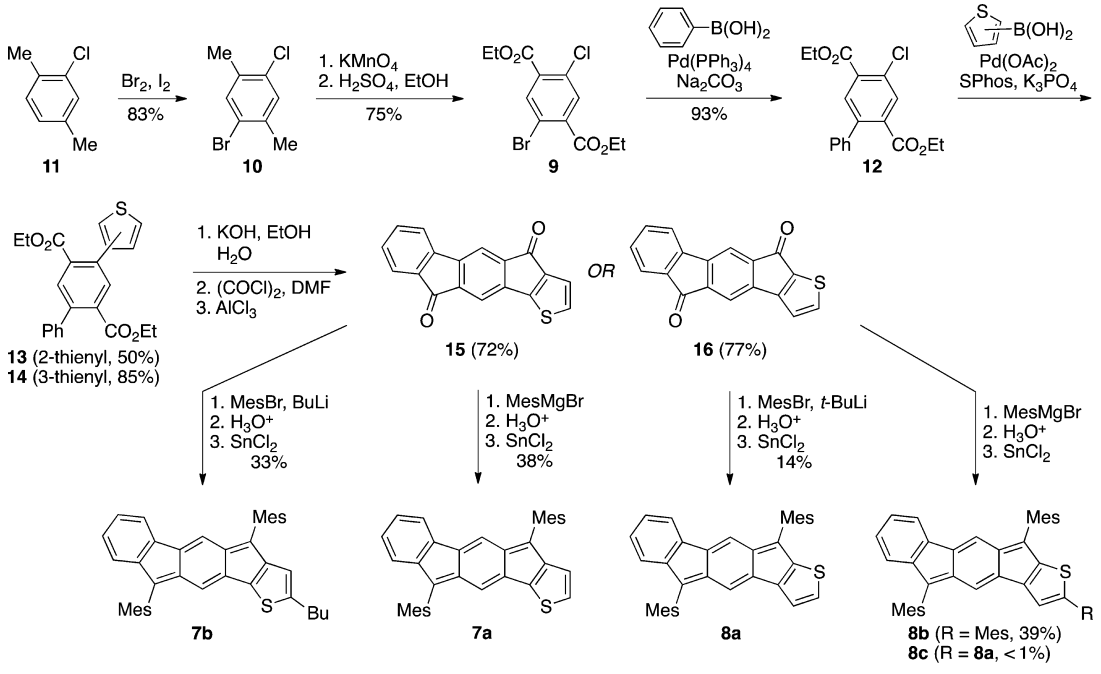

DOI: 10.1021/acs.joc.6b00340
J. Org. Chem. 2016, 81, 3674–3680

BIT **7b**. Similarly, treatment of **16** with mesityllithium (via *n*-BuLi and bromomesitylene) yielded an inseparable mixture of **8a** and the corresponding butylated product. Much to our surprise, treatment of **16** with mesitylmagnesium bromide did not furnish **8a**; rather, compound **8b** and trace amounts of BIT dimer **8c** were isolated. Although Grignard-mediated couplings of thiophenes are known,[54−56] the formation of **8b** and **8c** was nonetheless an unexpected result based on the lack of anomalous reactivity of **15** and the dione precursors of **2a−c** and **3a**,**b** to Grignard reagents. By preparing the mesityllithium reagent with *t*-BuLi, we were able to suppress the S_N2 reaction of any deprotonated dione and isolate pure **8a** albeit in reduced yield compared with **7a**.

Figure 3 shows the electronic absorption spectra for diones **15** and **16** (top) and BITs **7a** and **8a** (bottom). These data

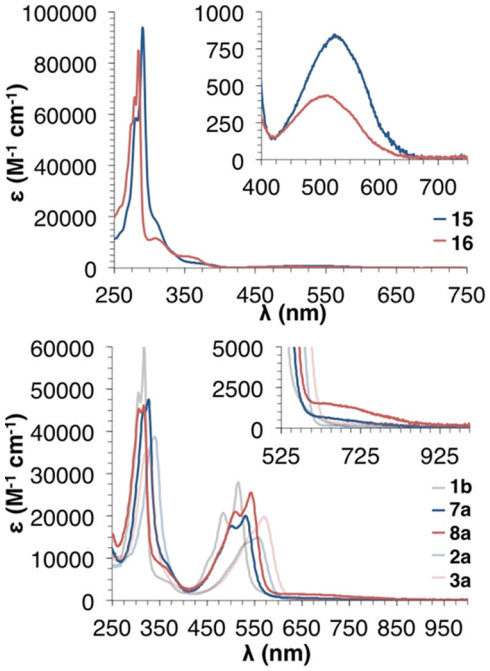

Figure 3. Electronic absorption spectra of BIT diones **15** and **16** (top) and of IF **1b** (R^1 = Mes, R^2 = H), *anti*-BIT **7a**, *syn*-BIT **8a**, *anti*-IDT **2a**, and *syn*-IDT **3a** (bottom).

along with the experimentally determined E^{redox} values, HOMO and LUMO energies, and energy gaps are summarized in Table 1. The spectra of diones **15** and **16** show strong absorptions from 275 to 325 nm with broad absorptions attributable to weak $\pi \rightarrow \pi^*$ transitions in the 450−600 nm range. The spectra of both fully conjugated BITs **7a** and **8a** show a maximum absorbance from 275 to 350 nm and a lower energy λ_{max} of 532 nm for **7a** and a λ_{max} of 543 nm for **8a**. Surprisingly, *syn*-BIT **8a** shows a weak tail out to 925 nm. The absorbance profiles of the BITs lie halfway between IF **1b** and the corresponding *syn*- or *anti*-IDT **2a** or **3a**, and as with all previous IFs and IDTs, BITs **7a** and **8a** are nonemissive.[57]

Both *anti*-BIT **7a** and *syn*-BIT **8a** undergo one reversible reduction in the solution state with the second reduction being irreversible (Figure 4). The first oxidations of **7a** and **8a** were

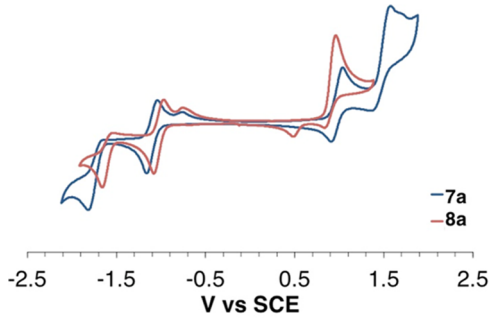

Figure 4. Cyclic voltammogram of *anti*-BIT **7a** and *syn*-BIT **8a**.

quasi-reversible and fully reversible, respectively, and the second oxidation of **8a** was quasi-reversible. For both **7a** and **8a**, when the current is swept through the second reduction, a new peak appears during the cathodic sweep of the CV scan (see Figures S1 and S2). This peak is absent when the current is not swept past the first reduction, indicating that this peak most likely arises from the reactive species created during the second reduction of **7a** and **8a**. As seen with the UV−vis spectra, the electrochemical behavior of the BITs lies between the IFs and IDTs. Although the E_{LUMO} of IF **1b**, *anti*-BIT **7a**, and *syn*-BIT **8a** are nearly the same (−3.56, −3.58, and −3.60 eV, respectively), the E_{HOMO} of **7a** and **8a** are stabilized when compared with IF **1b**. The resultant E_{gap} of BITs **7a** and **8a** (2.05 and 1.93 eV, respectively) lies between the E_{gap} of IF **1b** (2.22 eV) and IDTs **2a** and **3a** (1.88 and 1.85 eV, respectively).

Single crystals of **15**, **7a**,**b**, and **8a**,**b** suitable for X-ray diffraction (XRD) were grown by slow diffusion of CH_3CN into a solution of CH_2Cl_2, whereas single crystals of **8c** were grown by the slow evaporation of hexanes. The structures of **7a**, **8a**, and **8c** are shown in Figure 5 (see SI for **7b**, **8b**, and **15**). The crystal structures of **7a** and **8a** showed disorder over two centro-symmetrical positions corresponding to two opposite

Table 1. Electrochemical and Optical Data for BIT Diones 15 and 16 and BITs 7a and 8a

	electrochemical[a]							optical[b]		
compd	E_{red}^1 (V)	E_{red}^2 (V)	E_{ox}^1 (V)	E_{ox}^2 (V)	E_{HOMO} (eV)	E_{LUMO} (eV)	E_{gap} (eV)	λ_{max} (nm)	λ_{onset} (nm)	E_{gap} (eV)
15	−0.86	−1.29				−3.78		525	619	2.00
16	−0.83	−1.24				−3.81		510	610	2.03
7a	−1.06	−1.77[c]	0.99	1.61[c]	−5.63	−3.58	2.05	532	562	2.21
8a	−1.04	−1.68[c]	0.89		−5.53	−3.60	1.93	543	572	2.16

[a]Spectra were obtained in CH_2Cl_2. The optical HOMO/LUMO gap was determined as the intersection of the *x*-axis and a tangent line passing through the inflection point of the lowest energy absorption. [b]CVs were recorded using 1−5 mM of analyte in 0.1 M Bu_4NBF_4/CH_2Cl_2 at a scan rate of 50 mV s^{-1} with a glassy carbon working electrode, a Pt coil counter electrode, and a Ag wire pseudoreference. Values reported as the half-wave potential (vs SCE) using the Fc/Fc^+ couple (0.46 V) as an internal standard. HOMO and LUMO energy levels in eV were approximated using SCE = −4.68 eV vs vacuum and $E_{1/2}$ values for reversible processes or E_p values for irreversible processes. [c]Reported as V at peak current, not half-wave potential.

DOI: 10.1021/acs.joc.6b00340
J. Org. Chem. 2016, 81, 3674−3680

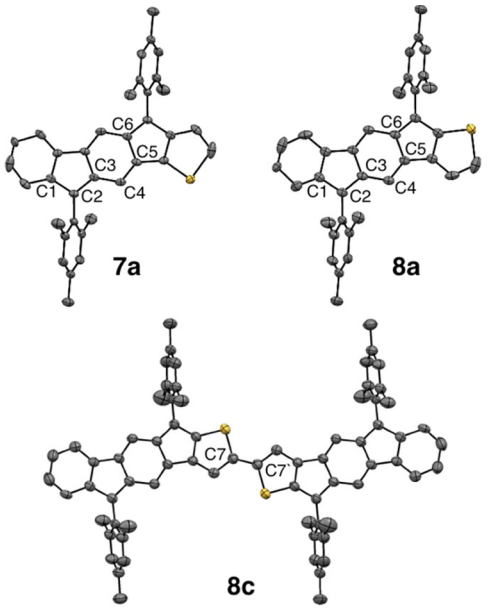

Figure 5. Molecular structures of **7a**, **8a**, and **8c**; hydrogen atoms are omitted for clarity. Ellipsoids are drawn at 50% probability level.

orientations, indicating that the dipole induced by desymmetrization was insufficient to direct the solid-state ordering of these compounds. A comparison of select bond lengths of the BITs (**7a**, **8a**) along with the dimesityl derivative of [1,2-*b*]IF **1b** and IDTs **2a** and **3a** are given in Table 2 (see Table S1 for

Table 2. Selected Bond Lengths (Å) For 7a, 8a, 1b, 2a, and 3a

	anti/syn-BIT		IF, *anti/syn*-IDT[b]		
bond[a]	**7a**	**8a**	**1b** (Mes)	**2a**	**3a**
C1−C2	1.468(4)	1.453(3)	1.471(3)	1.460(2)	1.447(3)
C2−C3	1.385(3)	1.388(2)	1.380(2)	1.388(2)	1.398(3)
C3−C4	1.427(3)	1.427(2)	1.433(3)	1.431(2)	1.418(3)
C4−C5	1.359(3)	1.361(2)	1.356(2)	1.360(2)	1.363(3)
C5−C6	1.463(4)	1.467(2)	1.467(3)	1.469(2)	1.456(3)

[a]Numbering scheme shown in Figure 5. [b]Numbering scheme for **1b**, **2a**, and **3a** is the same for **7a** and **8a** and is shown in Figure S4.

select bond lengths of **7b** and **8b**,**c**). All derivatives of **7** and **8** showed bond length alternation of the *s*-indacene core indicative of a quinoidal structure. From a bond length perspective, there were no significant structural differences between the BIT *syn/anti* isomers nor between indacene cores of the BITs, IDTs, or the dimesityl derivative of IF **1b**. The dihedral angle between the average planes of the mesityl groups and BIT core for **7a** (67.4°) and **8a** (69.9°) is similar to that of the mesityl derivative of **1b** (68.0°), **2a** (67.0°), and **3a** (62.2°). Interestingly, the structure of dimer **8c** shows co-planarity of the two BIT cores (0.0° angle between the average planes), and the thiophene−thiophene bond (C7−C7′) is 1.45 Å, which is in excellent agreement with the corresponding bond length reported for various oligothiophene dervatives (∼1.44−1.45 Å).[58−60] This information suggests electronic communication between the BIT cores of the dimer; further study is ongoing.

Both *anti*-BIT **7a** and *syn*-BIT **8a** pack in a herringbone-like manner (Figure 6). The sulfur of **7a** partakes in a close C−S contact of 3.37 Å, whereas the distance between the sulfur and

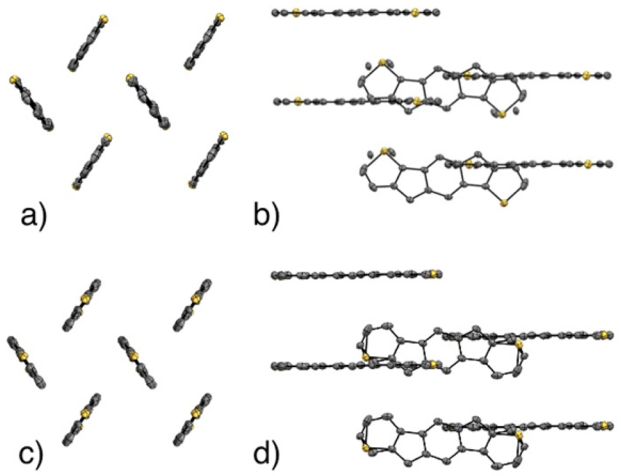

Figure 6. Packing diagrams of **7a** (a,b) and **8a** (c,d); hydrogen atoms and mesityl groups are omitted for clarity. Ellipsoids are drawn at 50% probability level.

the average plane of the *anti*-BIT core is 3.32 Å. Conversely, *syn*-BIT **8a** shows no close C−C or C−S contacts, and the shortest distance between the average plane of the syn-BIT core and the nearest adjacent molecule is 3.40 Å. *Syn*-BIT dimer **8c** packs in an expanded herringbone motif with no close C−C or C−S contacts and no overlap of the BIT core (see SI).

■ CONCLUSIONS

In summary, we have developed a modular synthetic route toward the synthesis of unsymmetric IFs and related compounds. This synthetic route allows us unprecedented regioselective control, and we have demonstrated the synthetic utility of this route by synthesizing two new unsymmetrical IF analogues: *anti*-BIT **7a** and *syn*-BIT **8a**. Optical and electrochemical characterization reveals that the BIT properties lie between those of the IFs and IDTs. With the synthetic utility of this route clearly demonstrated, we are now using this methodology to synthesize previously inaccessible IFs possessing strong dipole moments or cruciform topologies to exploit potential solid-state order or study the electronic nature of the indenofluorene core.

■ EXPERIMENTAL SECTION

General Remarks. All air-sensitive manipulations were carried out under an inert atmosphere using either standard Schlenk technique or a N_2-filled drybox. For air-sensitive reactions, THF and toluene were refluxed with Na benzophenone ketyl for 24 h prior to distillation and use. For all manipulations performed in a N_2-filled drybox, THF and toluene were refluxed with Na benzophenone ketyl for 24 h prior to distillation and then degassed via freeze−pump−thaw cycles. All other reagents were used as received without further purification. NMR spectra were recorded on a 300 and 500 MHz instrument and a 500 and 600 MHz instrument equipped with a cryoprobe. ^{1}H and ^{13}C chemical shifts (δ) are expressed in ppm relative to the residual $CHCl_3$ (^{1}H: 7.26 ppm, ^{13}C: 77.16 ppm) and DMSO (^{1}H: 2.50 ppm, ^{13}C: 39.52 ppm) references. UV−vis spectra were recorded on a UV−vis spectrometer in HPLC grade CH_2Cl_2.

*1-Bromo-4-chloro-2,5-dimethylbenzene (**10**).* 2-Chloro-1,4-dimethylbenzene (9.44 mL, 71.2 mmol, 1 equiv), iodine (0.091 g, 0.36 mmol, 0.005 equiv), and CH_2Cl_2 (100 mL) were degassed with N_2 for 15 min and cooled to 0 °C. Bromine (3.85 mL, 74.7 mmol, 1.05 equiv) was added dropwise, and the reaction mixture was stirred for 18 h in the dark while warming to room temperature. The reaction mixture was quenched with 10% KOH solution and then extracted

DOI: 10.1021/acs.joc.6b00340
J. Org. Chem. 2016, 81, 3674−3680

with CH_2Cl_2 (3×). The combined organic fractions were then washed with brine (3×), dried ($MgSO_4$), filtered, and concentrated in vacuo. The crude product was recrystallized from EtOH to yield **10** (12.9 g, 83%) as white crystals. Mp 66−67 °C. ^{1}H NMR (300 MHz, $CDCl_3$) δ 7.38 (s, 1H), 7.20 (s, 1H), 2.33 (s, 3H), 2.31 (s, 3H). ^{13}C NMR (126 MHz, $CDCl_3$) δ 136.8, 135.2, 134.2, 133.2, 130.9, 122.6, 22.4, 19.4. HRMS (TOF MS AP+) for C_8H_8ClBr: calcd 217.9498, found 217.9510.

*Diethyl 2-Bromo-5-chloroterephthalate (**9**).* 1-Bromo-4-chloro-2,5-dimethylbenzene **10** (12.77 g, 58.2 mmol, 1 equiv), $KMnO_4$ (20.23 g, 128 mmol, 2.2 equiv), H_2O (100 mL), and *t*-BuOH (100 mL) were stirred at reflux for 1 h. After cooling, additional $KMnO_4$ (20.23 g, 128 mmol, 2.2 equiv) was added, and the mixture was then refluxed for 18 h. After cooling, the mixture was filtered, and the diacid was precipitated by careful addition of concd HCl solution to yield 2-bromo-5-chloroterephthalic acid (14.84 g, 91%) as a white powder that was carried on without further purification. The crude diacid (14.84 g, 52.0 mmol, 1 equiv), concd H_2SO_4 (57 mL), and EtOH (400 mL) were stirred at reflux for 18 h. After cooling, EtOH was removed under reduced pressure. The reaction mixture was partially neutralized by the addition of saturated $NaHCO_3$ solution and then fully neutralized by careful addition of solid KOH pellets. The precipitate was collected via vacuum filtration and then dissolved in CH_2Cl_2 to separate the salts from the product. The solution was dried ($MgSO_4$) and filtered, and the solvent was removed under reduced pressure. Recrystallization of the crude material from EtOH furnished diester **9** (14.22 g, 82%) as brilliant white crystals. Mp 117−118 °C. ^{1}H NMR (500 MHz, $CDCl_3$) δ 8.07 (s, 1H), 7.83 (s, 1H), 4.41 (q, J = 7.2 Hz, 4H), 1.41 (t, J = 7.2 Hz, 6H). ^{13}C NMR (126 MHz, $CDCl_3$) δ 164.5, 163.8, 136.7, 135.9, 133.7, 133.4, 132.7, 119.3, 62.5, 62.4, 14.29, 14.27. HRMS (TOF MS FAB+) for $C_{12}H_{13}O_4ClBr$ $(M + H)^+$: calcd 334.9686, found 334.9670.

*Diethyl 2-Chloro-5-phenylterephthalate (**12**).* Diethyl 2-bromo-5-chloroterephthalate **9** (7.00 g, 20.9 mmol, 1 equiv), phenylboronic acid (3.05 g, 25.0 mmol, 1.2 equiv), Na_2CO_3 (4.42 g, 41.7 mmol, 2 equiv), H_2O (30 mL), and toluene (300 mL) were degassed for 60 min with N_2. $Pd(PPh_3)_4$ (0.482 g, 0.42 mmol, 0.02 equiv) was then added, and the resulting solution was degassed for a further 10 min. The mixture was then stirred at reflux for 18 h. After cooling, the mixture was quenched with H_2O and extracted with Et_2O (3×). The organic layers were combined, washed with brine (3×), dried ($MgSO_4$), filtered, and concentrated in vacuo. The product was purified via flash chromatography (SiO_2, 2:1 CH_2Cl_2/hexanes) to provide **12** (6.94 g, 93%) as a clear oil that slowly solidified to a white solid. Mp 55−56 °C. ^{1}H NMR (500 MHz, $CDCl_3$) δ 7.88 (s, 1H), 7.80 (s, 1H), 7.43−7.36 (m, 3H), 7.32−7.27 (m, 2H), 4.42 (q, J = 7.1 Hz, 2H), 4.11 (q, J = 7.1 Hz, 2H), 1.40 (t, J = 7.2 Hz, 3H), 1.01 (t, J = 7.2 Hz, 3H). ^{13}C NMR (126 MHz, $CDCl_3$) δ 166.9, 165.1, 140.9, 139.5, 134.8, 133.4, 132.6, 132.5, 132.1, 128.44, 128.36, 128.0, 62.1, 61.7, 14.3, 13.8. HRMS (TOF MS ES+) for $C_{18}H_{18}O_4Cl$ $(M + H)^+$: calcd 333.0894, found 333.0899.

*Diethyl 2-Phenyl-5-(2-thienyl)terephthalate (**13**).* An air-free oven-dried three-necked round-bottomed flask fitted with a condenser was charged with diester **12** (3.0 g, 9.01 mmol, 1 equiv), 2-thienylboronic acid (1.38 g, 10.8 mmol, 1.2 equiv), K_3PO_4, (3.825 g, 18.0 mmol, 2 equiv), SPhos ligand (0.148 g, 0.36 mmol, 0.04 equiv), and $Pd(OAc)_2$ (0.0405 g, 0.18 mmol, 0.02 equiv). Dry toluene (125 mL) was added to the flask, and N_2 was bubbled through the reaction mixture for 10 min. After refluxing overnight and cooling to room temperature, the reaction mixture was quenched with H_2O and extracted with Et_2O (3×). The combined organic layers were then washed with brine (3×), dried ($MgSO_4$), filtered, and concentrated in vacuo. The resultant crude yellow oil was purified via column chromatography (SiO_2, 19:1 hexanes/EtOAc) to yield diester **13** (1.70 g, 50%) as a fluffy white solid. Mp 74−75 °C. ^{1}H NMR (600 MHz, $CDCl_3$) δ 7.92 (s, 1H), 7.72 (s, 1H), 7.43−7.38 (m, 4H), 7.36−7.33 (m, 2H), 7.11 (dd, J = 3.5, 1.3 Hz, 1H), 7.08 (dd, J = 5.0, 3.6 Hz, 1H), 4.22 (q, J = 7.1 Hz, 2H), 4.11 (q, J = 7.1 Hz, 2H), 1.15 (t, J = 7.1 Hz, 3H), 1.01 (t, J = 7.2 Hz, 3H). ^{13}C NMR (151 MHz, $CDCl_3$) δ 168.1, 167.9, 141.8, 140.8, 140.1, 134.4, 133.5, 133.1, 132.4, 131.6, 128.5, 128.3, 127.8, 127.4, 127.0, 126.5, 61.7, 61.5, 14.0, 13.8. HRMS (TOF MS ES+) for $C_{22}H_{21}O_4S$ $(M + H)^+$: calcd 381.1161, found 381.1156.

*Diethyl 2-Phenyl-5-(3-thienyl)terephthalate (**14**).* The above procedure was followed using 3-thienylboronic acid instead. Recrystallization of the crude material from EtOH yielded diester **14** (2.92 g, 85%) as white needles. Mp 117−118 °C. ^{1}H NMR (600 MHz, $CDCl_3$) δ 7.85 (s, 1H), 7.76 (s, 1H), 7.45−7.34 (m, 6H), 7.32 (dd, J = 3.0, 1.3 Hz, 1H), 7.14 (dd, J = 4.9, 1.3 Hz, 1H), 4.19 (q, J = 7.1 Hz, 2H), 4.11 (q, J = 7.1 Hz, 2H), 1.14 (t, J = 7.1 Hz, 3H), 1.00 (t, J = 7.1 Hz, 3H). ^{13}C NMR (151 MHz, $CDCl_3$) δ 168.2, 168.1, 141.3, 140.29, 140.28, 135.6, 133.71, 133.66, 131.8, 131.7, 128.53, 128.51, 128.3, 127.7, 125.5, 123.0, 61.6, 61.5, 14.0, 13.8. HRMS (TOF MS ES+) for $C_{22}H_{21}O_4S$ $(M + H)^+$: calcd 381.1161, found 381.1178.

General Procedure for Dione Synthesis. Diester (1 equiv) and KOH (16 equiv) were refluxed in a 4:1 mixture of EtOH and H_2O (0.03 M) for 18 h. The EtOH was removed under reduced pressure and after cooling to 0 °C; the diacid was precipitated by careful addition of concd HCl solution. The solid was collected by filtration, washed with water, and dried. The crude diacid was carried on without further characterization. To a stirred suspension of crude diacid (1 equiv) and oxalyl chloride (4 equiv) in dry CH_2Cl_2 (0.04 M) at 0 °C under a N_2 atmosphere in an oven-dried flask was added DMF (2 equiv) dropwise. The reaction mixture was warmed slowly to room temperature with stirring over 6 h, and then was evaporated to dryness under reduced pressure. The crude acid chloride was redissolved in dry CH_2Cl_2 (0.08 M) and cooled to 0 °C under N_2. A 0 °C solution of $AlCl_3$ (2.62 g, 19.65 mmol, 5 equiv) in dry CH_2Cl_2 (0.4 M) was transferred to the crude acid chloride solution via cannula, and the resulting mixture was warmed to room temperature overnight with stirring. This solution was then poured into an HCl/ice mixture, and the resulting dione was collected via vacuum filtration, washed with H_2O, EtOH, hexanes, and acetone and then oven-dried at 70 °C.

*anti-Dione **15**.* Cerulean blue solid (0.871 g, 72% over 3 steps). Mp 334−335 °C, 330 °C (sub). ^{1}H NMR (500 MHz, $CDCl_3$) δ 7.65 (d, J = 7.5 Hz, 1H), 7.63 (s, 1H), 7.56−7.48 (m, 2H), 7.42 (s, 1H), 7.33 (t, J = 7.2 Hz, 1H), 7.24 (d, J = 5.2 Hz, 1H), 7.17 (d, J = 5.0 Hz, 1H). ^{13}C NMR (126 MHz, $CDCl_3$) δ 192.8, 186.0, 158.6, 146.3, 143.6, 142.2, 142.0, 139.9, 138.6, 135.4, 133.8, 130.1, 129.6, 124.6, 121.8, 120.6, 115.9, 114.9. UV−vis (CH_2Cl_2) λ_{max} (ε) 284 (58100), 290 (93900), 525 (850) nm. HRMS (TOF MS AP−) for $C_{18}H_8O_2S$: calcd 288.0245, found 288.0230.

*syn-Dione **16**.* Cerulean blue solid (1.599 g, 77% over 3 steps). Mp 325−326 °C. ^{1}H NMR (500 MHz, $CDCl_3$) δ 7.84 (d, J = 4.5 Hz, 1H), 7.70−7.63 (m, 2H), 7.56−7.49 (m, 2H), 7.47 (s, 1H), 7.33 (t, J = 7.2 Hz, 1H), 7.18 (d, J = 4.5 Hz, 1H). ^{13}C NMR (151 MHz, $CDCl_3$) δ 193.1, 184.3, 158.2, 146.0, 143.7, 143.6, 140.9, 140.6, 138.4, 137.0, 135.4, 133.8, 129.5, 124.6, 120.6, 120.5, 116.3, 115.2. UV−vis (CH_2Cl_2) λ_{max} (ε) 281 (63900), 284 (84900), 510 (430) nm. HRMS (TOF MS AP−) for $C_{18}H_8O_2S$: calcd 288.0245, found 288.0254.

General Procedure for BIT Synthesis. To a stirred suspension of dione (1 equiv) in THF (0.01 M) at 0 °C under a N_2 atmosphere was added mesitylmagnesium bromide (1.0 M in THF, 6 equiv) dropwise. The mixture was then slowly warmed to rt with stirring overnight. The reaction was quenched with a saturated NH_4Cl solution and then extracted with Et_2O (3×). The combined organic fractions were then washed with brine (3×), dried ($MgSO_4$), filtered, and then concentrated in vacuo to provide the crude diol that was carried on without further purification.

In an oven-dried flask in a N_2 drybox, the crude diol (1 equiv) was dissolved in dry, degassed toluene (0.02 M) and vigorously stirred with anhydrous $SnCl_2$ (4 equiv) for 14 h. The reaction mixture was then filtered through a short plug of silica gel (CH_2Cl_2). After removing the solvent in vacuo, the crude product was purified via flash chromatography (SiO_2, 4:1 hexanes/CH_2Cl_2) to yield the desired BIT.

*anti-BIT **7a**.* Deep purple solid (324 mg, 38%). Mp 342−343 °C, 337 °C (sub). ^{1}H NMR (600 MHz, $CDCl_3$) δ 7.13 (d, J = 7.2 Hz, 1H), 6.99 (s, 2H), 6.98 (s, 2H), 6.93−6.89 (m, 2H), 6.82 (td, J = 7.4, 1.1 Hz, 1H), 6.58 (d, J = 7.6 Hz, 1H), 6.52 (s, 1H), 6.47 (s, 1H), 6.38 (d, J = 4.8 Hz, 1H), 2.37 (s, 3H), 2.37 (s, 3H), 2.27 (s, 6H), 2.18 (s,

DOI: 10.1021/acs.joc.6b00340
J. Org. Chem. 2016, 81, 3674−3680

6H). ^{13}C NMR (151 MHz, $CDCl_3$) δ 151.9, 148.4, 144.0, 142.0, 139.21, 139.17, 137.8, 137.6, 137.1, 137.0, 136.1, 136.0, 135.9, 135.1, 130.7, 129.9, 128.4, 128.3, 127.9, 127.8, 127.3, 122.5, 121.2, 120.6, 120.3, 120.1, 21.32, 21.31, 20.7, 20.6. UV−vis (CH_2Cl_2) λ_{max} (ε) 318 (44700), 327 (47500), 504 (17550), 532 (20000) nm. HRMS (TOF MS ES+) for $C_{36}H_{31}S$ (M + H)$^+$: calcd 495.2133, found 495.2146.

anti-BIT ***7b***. An oven-dried flask charged with bromomesitylene (0.63 mL, 4.14 mmol, 6 equiv) and dry THF (25 mL) under N_2 was cooled to −78 °C, and BuLi (1.6 M in hexanes, 2.16 mL, 3.45 mmol, 5 equiv) was added dropwise. After stirring at −78 °C for 1 h, the mixture was transferred via cannula to an oven-dried flask charged with dione **15** (200 mg, 0.69 mmol, 1 equiv) in THF (25 mL) at 0 °C under a N_2 atmosphere. The mixture was stirred while slowly warming to room temperature. After 3 d, the reaction was worked up following the general procedure. Treatment of the crude diol following the general procedure furnished pure *anti*-BIT **7b** (125 mg, 33%) as bright purple crystals. Mp 248−249 °C. ^{1}H NMR (600 MHz, $CDCl_3$) δ 7.08 (d, J = 7.3 Hz, 1H), 6.98 (s, 2H), 6.97 (s, 2H), 6.88 (d, J = 7.7 Hz, 1H), 6.79 (d, J = 7.7 Hz, 1H), 6.54 (d, J = 7.5 Hz, 1H), 6.45 (s, 1H), 6.34 (s, 1H), 6.08 (s, 1H), 2.61 (t, J = 7.6 Hz, 2H), 2.37 (s, 3H), 2.36 (s, 3H), 2.27 (s, 6H), 2.18 (s, 6H), 1.59−1.51 (m, 2H), 1.33 (sext, J = 7.4 Hz, 2H), 0.88 (t, J = 7.4 Hz, 3H). ^{13}C NMR (151 MHz, $CDCl_3$) δ 151.5, 149.6, 147.9, 144.1, 142.5, 139.3, 137.7, 137.5, 137.1, 137.0, 136.8, 136.7, 135.5, 135.4, 135.3, 130.8, 130.0, 128.34, 128.27, 127.8, 127.1, 122.4, 120.5, 120.3, 119.9, 117.8, 33.5, 30.5, 22.2, 21.3, 20.7, 20.6, 13.93. UV−vis (CH_2Cl_2) λ_{max} (ε) 331 (51100), 506 (19900), 536 (21800) nm. HRMS (TOF MS ES+) for $C_{40}H_{39}S$ (M + H)$^+$: calcd 551.2772, found 551.2765.

syn-BIT ***8a***. An oven-dried flask charged with bromomesitylene (0.40 mL, 2.6 mmol, 5 equiv) and dry THF (25 mL) under N_2 was cooled to −78 °C, and *t*-BuLi (1.7 M in hexanes, 1.84 mL, 3.1 mmol, 6 equiv) was added dropwise. After being stirred at −78 °C for 1 h, the mixture was transferred via cannula to an oven-dried flask charged with dione **16** (150 mg, 0.52 mmol, 1 equiv) in THF (25 mL) at −78 °C under a N_2 atmosphere. The mixture was stirred while slowly warming to room temperature overnight. The reaction was worked up following the general procedure. Treatment of the crude diol following the general procedure furnished pure *syn*-BIT **8a** (34.7 mg, 14%) as a deep purple solid. Mp 335−336 °C, 323 °C (sub). ^{1}H NMR (600 MHz, $CDCl_3$) δ 7.13 (d, J = 7.3 Hz, 1H), 7.02 (s, 2H), 7.01 (s, 2H), 6.98 (d, J = 4.8 Hz, 1H), 6.92 (td, J = 7.4, 1.0 Hz, 1H), 6.85−6.80 (m, 2H), 6.59 (d, J = 7.3 Hz, 1H), 6.534 (s, 1H), 6.528 (s, 1H), 2.40 (s, 3H), 2.39 (s, 3H), 2.33 (s, 6H), 2.21 (s, 6H). ^{13}C NMR (151 MHz, $CDCl_3$) δ 148.7, 148.0, 143.82, 143.78, 141.1, 139.0, 137.8, 137.6, 137.0, 136.9, 136.1, 135.8, 135.2, 135.0, 129.93, 129.87, 128.6, 128.3, 128.1, 127.8, 127.1, 122.4, 121.5, 120.10, 120.05, 119.96, 21.2, 20.5, 20.41. UV−vis (CH_2Cl_2) λ_{max} (ε) 308 (45100), 316 (46100), 510 (21000), 543 (25500) nm. HRMS (TOF MS ES+) for $C_{36}H_{31}S$ (M + H)$^+$: calcd 495.2146, found 495.2172.

syn-BIT ***8b*** *and syn-BIT dimer* ***8c***. Following the general procedure, dione **16** yielded a mixture of **8b** and **8c**. Column chromatography (SiO_2, 6:1 hexanes/CH_2Cl_2) afforded pure material with **8b** eluting first and **8c** eluting second. **8b**: maroon solid (99.3 mg, 39%). Mp 220−222 °C. ^{1}H NMR (600 MHz, $CDCl_3$) δ 7.11 (d, J = 7.5 Hz, 1H), 6.98 (s, 4H), 6.92−6.88 (m, 3H), 6.80 (d, J = 7.2 Hz, 1H), 6.56 (d, J = 7.5 Hz, 1H), 6.52−6.49 (m, 3H), 2.36 (s, 12H), 2.29 (s, 3H), 2.21−2.16 (m, 12H). ^{13}C NMR (151 MHz, $CDCl_3$) δ 148.7, 148.0, 145.7, 144.0, 143.9, 141.8, 139.3, 138.4, 138.1, 137.9, 137.7, 137.1, 137.0, 136.7, 135.6, 135.2, 134.5, 131.4, 130.2, 130.1, 128.5, 128.3, 127.9, 127.1, 122.5, 121.8, 120.3, 120.2, 120.0, 21.3, 21.2, 20.9, 20.7, 20.6. UV−vis (CH_2Cl_2) λ_{max} (ε) 310 (43800), 319 (44200), 518 (19300), 551 (22800) nm. HRMS (TOF MS ES+) for $C_{45}H_{41}S$ (M + H)$^+$: calcd 613.2929, found 613.2900. **8c**: dark purple solid (<1.0 mg, <1%). Mp >340 °C. ^{1}H NMR (500 MHz, THF-d_8) δ 7.18 (d, J = 7.5 Hz, 2H), 7.05 (s, 2H), 6.97 (s, 4H), 6.95 (s, 4H), 6.85 (t, J = 7.6 Hz, 2H), 6.76 (t, J = 7.5 Hz, 2H), 6.59 (s, 2H), 6.52 (s, 2H), 6.50 (d, J = 7.8 Hz, 2H), 2.32 (s, 6H), 2.31 (s, 6H), 2.26 (s, 12H), 2.13 (s, 12H). Extremely low solubility precluded ^{13}C NMR analysis. UV−vis (CH_2Cl_2) λ_{max} (ε) 320, 383, 587, 890 (br), 1000 (sh) nm. HRMS (TOF MS ES+) for $C_{72}H_{58}S_2$ (M + H)$^+$: calcd 986.3980, found 986.3989.

■ ASSOCIATED CONTENT

Ⓢ Supporting Information

The Supporting Information is available free of charge on the ACS Publications Web site at DOI: 10.1021/acs.joc.XXXXXXX. (PDF) The Supporting Information is available free of charge on the ACS Publications website at DOI: 10.1021/acs.joc.6b00340.

^{1}H and ^{13}C NMR spectra for all new compounds, CV and X-ray crystallographic data, and a bond length comparison for **7b**, **8b**, and **8c** (PDF)
Crystallographic information for **7a** (CIF)
Crystallographic information for **7b** (CIF)
Crystallographic information for **8a** (CIF)
Crystallographic information for **8b** (CIF)
Crystallographic information for **8c** (CIF)
Crystallographic information for **15** (CIF)

■ AUTHOR INFORMATION

Corresponding Author

*E-mail: haley@uoregon.edu.

Notes

The authors declare no competing financial interest.

■ ACKNOWLEDGMENTS

We thank the National Science Foundation (CHE-1301485) for support of the research as well as support in the form of an instrumentation grant (CHE-1427987). HRMS data were obtained at the Mass Spectrometry Facilities and Services Core of the Environmental Health Sciences Center, Oregon State University, supported by grant #L30-CS00210, National Institute of Environmental Health Sciences, National Institutes of Health.

■ REFERENCES

(1) Chase, D. T.; Fix, A. G.; Kang, S. J.; Rose, B. D.; Weber, C. D.; Zhong, Y.; Zakharov, L. N.; Lonergan, M. C.; Nuckolls, C.; Haley, M. M. *J. Am. Chem. Soc.* **2012**, *134*, 10349−10352.
(2) Chase, D. T.; Fix, A. G.; Rose, B. D.; Weber, C. D.; Nobusue, S.; Stockwell, C. E.; Zakharov, L. N.; Lonergan, M. C.; Haley, M. M. *Angew. Chem., Int. Ed.* **2011**, *50*, 11103−11106.
(3) Chase, D. T.; Rose, B. D.; McClintock, S. P.; Zakharov, L. N.; Haley, M. M. *Angew. Chem., Int. Ed.* **2011**, *50*, 1127−1130.
(4) Fix, A. G.; Chase, D. T.; Haley, M. M. *Top. Curr. Chem.* **2012**, *349*, 159−195.
(5) Fix, A. G.; Deal, P. E.; Vonnegut, C. L.; Rose, B. D.; Zakharov, L. N.; Haley, M. M. *Org. Lett.* **2013**, *15*, 1362−1365.
(6) Frederickson, C. K.; Haley, M. M. *J. Org. Chem.* **2014**, *79*, 11241−11245.
(7) Marshall, J. L.; Haley, M. M. In *Organic Redox Systems: Synthesis, Properties and Applications*; Nishinaga, T., Ed.; Wiley: New York, 2016; pp 311−358.
(8) Marshall, J. L.; Rudebusch, G. E.; Vonnegut, C. L.; Zakharov, L. N.; Haley, M. M. *Tetrahedron Lett.* **2015**, *56*, 3235−3239.
(9) Rose, B. D.; Chase, D. T.; Weber, C. D.; Zakharov, L. N.; Lonergan, M. C.; Haley, M. M. *Org. Lett.* **2011**, *13*, 2106−2109.
(10) Rose, B. D.; Maria, P. J. S.; Fix, A. G.; Vonnegut, C. L.; Zakharov, L. N.; Parkin, S. R.; Haley, M. M. *Beilstein J. Org. Chem.* **2014**, *10*, 2122−2130.
(11) Rose, B. D.; Sumner, N. J.; Filatov, A. S.; Peters, S. J.; Zakharov, L. N.; Petrukhina, M. A.; Haley, M. M. *J. Am. Chem. Soc.* **2014**, *136*, 9181−9189.

DOI: 10.1021/acs.joc.6b00340
J. Org. Chem. 2016, 81, 3674−3680

(12) Rose, B. D.; Vonnegut, C. L.; Zakharov, L. N.; Haley, M. M. *Org. Lett.* **2012**, *14*, 2426−2429.
(13) Rudebusch, G. E.; Fix, A. G.; Henthorn, H. A.; Vonnegut, C. L.; Zakharov, L. N.; Haley, M. M. *Chem. Sci.* **2014**, *5*, 3627−3633.
(14) Young, B. S.; Chase, D. T.; Marshall, J. L.; Vonnegut, C. L.; Zakharov, L. N.; Haley, M. M. *Chem. Sci.* **2014**, *5*, 1008−1014.
(15) Miyoshi, H.; Nobusue, S.; Shimizu, A.; Hisaki, I.; Miyata, M.; Tobe, Y. *Chem. Sci.* **2014**, *5*, 163−168.
(16) Shi, X.; Burrezo, P. M.; Lee, S.; Zhang, W.; Zheng, B.; Dai, G.; Chang, J.; Lopez Navarrete, J. T.; Huang, K.-W.; Kim, D.; Casado, J.; Chi, C. *Chem. Sci.* **2014**, *5*, 4490−4503.
(17) Shimizu, A.; Kishi, R.; Nakano, M.; Shiomi, D.; Sato, K.; Takui, T.; Hisaki, I.; Miyata, M.; Tobe, Y. *Angew. Chem., Int. Ed.* **2013**, *52*, 6076−6079.
(18) Shimizu, A.; Nobusue, S.; Miyoshi, H.; Tobe, Y. *Pure Appl. Chem.* **2014**, *86*, 517−528.
(19) Shimizu, A.; Tobe, Y. *Angew. Chem., Int. Ed.* **2011**, *50*, 6906−6910.
(20) Takeda, T.; Inukai, K.; Tahara, K.; Tobe, Y. *J. Org. Chem.* **2011**, *76*, 9116−9121.
(21) Tobe, Y. *Chem. Rec.* **2015**, *15*, 86−96.
(22) Fukuda, K.; Nagami, T.; Fujiyoshi, J.-y.; Nakano, M. *J. Phys. Chem. A* **2015**, *119*, 10620−10627.
(23) Martinez, I.; Zarate, X.; Schott, E.; Morales-Verdejo, C.; Castillo, F.; Manríquez, J. M.; Chávez, I. *Chem. Phys. Lett.* **2015**, *636*, 31−34.
(24) Rao, M. R.; Desmecht, A.; Perepichka, D. F. *Chem. - Eur. J.* **2015**, *21*, 6193−6201.
(25) Sbargoud, K.; Mamada, M.; Marrot, J.; Tokito, S.; Yassar, A.; Frigoli, M. *Chem. Sci.* **2015**, *6*, 3402−3409.
(26) Zhang, X.-Y.; Huang, J.-D.; Yu, J.-J.; Li, P.; Zhang, W.-P.; Frauenheim, T. *Phys. Chem. Chem. Phys.* **2015**, *17*, 25463−25470.
(27) *Organic Light Emitting Devices: Synthesis, Properties and Applications*; Mullen, K., Scherf, U., Eds.; Wiley-VCH: Weinheim, Germany, 2006.
(28) *Carbon-rich Compounds: From Molecules to Materials*; Haley, M. M., Tykwinski, R. R., Eds.; Wiley-VCH: Weinheim, Germany, 2006.
(29) *Functional Organic Materials*; Muller, T. J. J., Bunz, U. H., Eds.; Wiley-VCH: Weinheim, Germany, 2007.
(30) *Fullerenes: Principles and Applications*; Langa, F., Nierengarten, J. F., Eds.; Royal Society of Chemistry: Cambridge, United Kingdom, 2011.
(31) *Fullerenes and Other Carbon-Rich Nanostructures*; Nierengarten, J. F., Ed.; Springer: Berlin, Germany, 2014.
(32) Anthony, J. E. *Chem. Rev.* **2006**, *106*, 5028−5048.
(33) Anthony, J. E. *Angew. Chem., Int. Ed.* **2008**, *47*, 452−483.
(34) Anthony, J. E.; Brooks, J. S.; Eaton, D. L.; Parkin, S. R. *J. Am. Chem. Soc.* **2001**, *123*, 9482−9483.
(35) Anthony, J. E.; Facchetti, A.; Heeney, M.; Marder, S. R.; Zhan, X. *Adv. Mater.* **2010**, *22*, 3876−3892.
(36) Clar, E. *Polycyclic Hydrocarbons*; Academic: London, United Kingdom, 1964.
(37) Dong, H.; Fu, X.; Liu, J.; Wang, Z.; Hu, W. *Adv. Mater.* **2013**, *25*, 6158−6183.
(38) Dong, H.; Wang, C.; Hu, W. *Chem. Commun.* **2010**, *46*, 5211−5222.
(39) Harvey, R. G. *Polycyclic Aromatic Hydrocarbons*; Wiley: New York, United States, 1997.
(40) Miao, Q. *Synlett* **2012**, *23*, 326−336.
(41) Anthony, J. E. In *Functional Organic Materials: Syntheses, Strategies and Applications*; Muller, T. J. J., Bunz, U. H. F., Eds.; Wiley-VCH: Weinheim, Germany, 2007; pp 511−545.
(42) Anthony, J. E. *Nat. Mater.* **2014**, *13*, 773−775.
(43) Lei, T.; Zhou, Y.; Cheng, C.-Y.; Cao, Y.; Peng, Y.; Bian, J.; Pei, J. *Org. Lett.* **2011**, *13*, 2642−2645.
(44) Swartz, C. R.; Parkin, S. R.; Bullock, J. E.; Anthony, J. E.; Mayer, A. C.; Malliaras, G. G. *Org. Lett.* **2005**, *7*, 3163−3166.
(45) Tang, M. L.; Okamoto, T.; Bao, Z. *J. Am. Chem. Soc.* **2006**, *128*, 16002−16003.
(46) Tang, M. L.; Reichardt, A. D.; Miyaki, N.; Stoltenberg, R. M.; Bao, Z. *J. Am. Chem. Soc.* **2008**, *130*, 6064−6065.
(47) Tang, M. L.; Reichardt, A. D.; Okamoto, T.; Miyaki, N.; Bao, Z. *Adv. Funct. Mater.* **2008**, *18*, 1579−1585.
(48) Tang, M. L.; Reichardt, A. D.; Siegrist, T.; Mannsfeld, S. C. B.; Bao, Z. *Chem. Mater.* **2008**, *20*, 4669−4676.
(49) Tang, M. L.; Reichardt, A. D.; Wei, P.; Bao, Z. *J. Am. Chem. Soc.* **2009**, *131*, 5264−5273.
(50) Valiyev, F.; Hu, W.-S.; Chen, H.-Y.; Kuo, M.-Y.; Chao, I.; Tao, Y.-T. *Chem. Mater.* **2007**, *19*, 3018−3026.
(51) Willgerodt, C.; Wolfien, R. *J. Prakt. Chem.* **1889**, *39*, 402−412.
(52) Varma, P. S.; Rman, K. S. V. *J. Indian Chem. Soc.* **1935**, *12*, 245−248.
(53) No attempt was made to optimize the Suzuki reactions as the literature precedents worked as described.
(54) Cahiez, G.; Duplais, C.; Buendia, J. *Angew. Chem., Int. Ed.* **2009**, *48*, 6731−6734.
(55) Cunningham, D. D.; Laguren-Davidson, L.; Mark, H. B.; Van Pham, C.; Zimmer, H. *J. Chem. Soc., Chem. Commun.* **1987**, 1021.
(56) Moglie, Y.; Mascaró, E.; Nador, F.; Vitale, C.; Radivoy, G. *Synth. Commun.* **2008**, *38*, 3861−3874.
(57) Rose, B. D.; Shoer, L. E.; Wasielewski, M. R.; Haley, M. M. *Chem. Phys. Lett.* **2014**, *616*−*617*, 137−141.
(58) Casado, J.; Hernández, V.; Hotta, S.; López Navarrete, J. T. *J. Chem. Phys.* **1998**, *109*, 10419.
(59) Chaloner, P. A.; Gunatunga, S. R.; Hitchcock, P. B. *Acta Crystallogr., Sect. C: Cryst. Struct. Commun.* **1994**, *50*, 1941−1942.
(60) Pelletier, M.; Brisse, F. *Acta Crystallogr., Sect. C: Cryst. Struct. Commun.* **1994**, *50*, 1942−1945.

DOI: 10.1021/acs.joc.6b00340
J. Org. Chem. 2016, 81, 3674−3680